

## DESIGN, PROCESSING AND PROPERTIES OF PRECIPITATION-HARDENABLE COMPLEX CONCENTRATED ALLOY

<sup>1,2</sup>Kateryna ULYBKINA, <sup>1</sup>Juraj LAPIN, <sup>1</sup>Kateryna KAMYSHNYKOVA

<sup>1</sup>*Institute of Materials and Machine Mechanics, Slovak Academy of Sciences, Bratislava, Slovakia, EU, [kateryna.ulybkina@savba.sk](mailto:kateryna.ulybkina@savba.sk)*

<sup>2</sup>*Faculty of Materials Science and Technology in Trnava, Slovak University of Technology, Trnava, Slovakia, EU*

<https://doi.org/10.37904/metal.2023.4689>

### Abstract

Complex concentrated alloy (CCA) with nominal composition (CoCrFeNi)<sub>92.5</sub>Al<sub>3</sub>Ti<sub>4.5</sub> (in at.%) was prepared by vacuum induction melting in a ceramic crucible and tilt cast into the cylindrical ceramic mould. The alloying elements such as Al and Ti were added to the basic quaternary CoCrFeNi system to promote the formation of L<sub>12</sub> phase in the FCC (face - centered cubic) matrix during heat treatments. The as-cast ingot was subjected to solid solution annealing, which was followed by free hot forging to refine the coarse columnar grain structure of the as-cast ingot. The forged alloy was subjected to annealing at 800 and 850 °C for 15 h. The properties of the CCA were studied with light microscopy (LM), energy dispersive spectroscopy (EDS), X-ray diffraction (XRD), nanohardness and microhardness measurements. The CCA solidifies through FCC(A1) primary solidification phase. The as-cast microstructure of the alloy consists of columnar dendritic grains growing from the surface towards the center of the cylindrical ingot. Solution annealing leads to a full chemical homogenization of the alloy and the formation of single-phase coarse columnar grains. Forging leads to the recrystallisation process and formation of equiaxed grains in the forgings. The annealing at the temperatures of 800 and 850 °C leads to significant hardening of the studied alloy, which is associated with the precipitation of L<sub>12</sub> particles in the FCC(A1) matrix.

**Keywords:** Complex concentrated alloy, casting, forging, heat treatments, hardening

### 1. INTRODUCTION

Since the discovery of high entropy alloys (HEAs) by Cantor et al. [1,2] and Yeh et al. [3], the systems with face-centered cubic (FCC) crystal structures became of large research interest because of their high strain hardening coefficients and excellent ductility at cryogenic temperatures [4]. The unique combination of properties of HEAs is achieved by mixing five or more elements in equal atomic proportions [5]. Mechanical properties of single-phase HEAs are controlled only by three strengthening mechanisms: (i) solid solution hardening, (ii) work-hardening and (iii) grain size [6,7]. These mechanisms become less effective at high temperatures due to recovery, recrystallisation, grain growth, and diffusive drag of solute atoms which leads to a significant softening and insufficient strength for structural applications. However, the best balance of strength and damage tolerance is found in structural materials that rely on significant volume fractions of intermetallic or ceramic phases [8-10]. To cover also the scope of microstructural complexity associated with multiphase alloys in the central regions of multi-dimensional phase diagrams, Gorse et al. [8,11] have introduced a concept of complex concentrated alloys (CCAs). The CCAs are also compositionally complex alloys but the rules concerning the number of elements and coexisting phases, concentration range, and magnitude or importance of configurational entropy satisfy not only to HEA definition but also include many other alloys including concentrated ternary and quaternary alloys. It has been reported that CCAs based on quaternary Co-Cr-Fe-Ni can serve as a good base for the design of CCAs strengthened by intermetallic and

ceramic phases for high-temperature structural applications [12]. He et al. [13] have reported outstanding tensile properties of the alloy with nominal composition  $(\text{FeCoNiCr})_{94}\text{Ti}_2\text{Al}_4$  (at.%), which has been achieved by precipitation of nanosized  $\text{L}_{12}\text{-Ni}_3(\text{Ti, Al})$  particles in CoCrFeNi HEA matrix.

The present work aims to design precipitation hardenable CCA based on Al-Co-Cr-Fe-Ni-Ti strengthened with  $\text{L}_{12}$  type precipitates, develop appropriate metallurgical routes for its processing and characterise some selected microstructural and mechanical properties.

## 2. EXPERIMENTAL PROCEDURE

The studied CCA with a nominal composition of  $(\text{CoCrFeNi})_{92.5}\text{Al}_3\text{Ti}_{4.5}$  (in at.%) was prepared by vacuum induction melting (VIM) of pure elements (purity 99.5 %) in pure  $\text{Al}_2\text{O}_3$  crucible placed into a protective alumina crucible equipped with a pouring cup connected to a cylindrical  $\text{Al}_2\text{O}_3$ -based mould. Before melting, the vacuum chamber of the induction furnace was evacuated to a vacuum pressure of 4.8 Pa, flushed with argon three times and finally partially filled with argon to a vacuum pressure of 10 kPa to minimise evaporation loss of Al during melting. The charge was heated to a melt temperature of 1580 °C and held at this temperature for 10 min to achieve full dissolution of all alloying elements. The temperature of the melt was measured by a pyrometer. The alloy was tilt-cast into the  $\text{Al}_2\text{O}_3$ -based mould. The as-cast ingots were subjected to solution annealing at a temperature of 1240 °C for 6 h under a protective dynamic argon atmosphere to homogenise their microstructure and chemistry before forging and further heat treatments. The forging experiments were conducted on solution-annealed ingots using a friction screw press. The annealing experiments were carried out at 800 and 850 °C for 15 h in air. After the annealing, the samples were quenched into the water at a temperature of 20 °C.

Metallographic preparation of the samples consisted of standard grinding using abrasive papers and polishing on diamond pastes with various grain sizes up to 0.25  $\mu\text{m}$ . The final polishing step was carried out electrolytically in a solution composed of 70 % ethanol, 20 % glycerin and 10 % perchloric acid at a temperature of -20 °C and voltage of 5 V. Microstructure evaluation was performed by light microscopy (LM), scanning electron microscopy (SEM) in backscattered electron (BSE) mode and energy-dispersive X-ray spectroscopy (EDS). The morphology and grain size were measured on digitalised micrographs using a computer image analyser and the software SigmaScanPro. The measured microstructural data were treated by statistical methods. The X-ray diffraction (XRD) analysis of coexisting phases was carried out by a diffractometer Bruker D8 equipped with an X-ray tube with a rotating Cu anode operating at 12 kW.

The Vickers microhardness of the samples was measured using a ZHV $\mu$  Vickers tester with an applied load of 0.49 N and 10 s dwell time. Each sample was measured 50 times, and then all the hardness values were averaged to achieve the final mean microhardness. Instrumented nanoindentation testing was carried out at an applied load of 0.01 N and holding time at the point of load application of 5 s on polished and slightly etched samples using universal nanomechanical testing system Zwick/Roell ZHN with Berkovich tip of the indenter.

## 3. RESULTS AND DISCUSSION

### 3.1 Microstructure and chemical composition of as-cast CCA

**Figure 1** shows the typical microstructure of the as-cast  $(\text{CoCrFeNi})_{92.5}\text{Al}_3\text{Ti}_{4.5}$  CCA. The microstructure consists of coarse columnar grains with an average grain diameter of  $(2.1 \pm 0.5)$  mm and an average grain length of  $(8.5 \pm 0.6)$  mm. The microstructure of the columnar grains consists of dendrites (78 vol.%) and interdendritic region (22 vol.%), as seen in **Figure 1a** and **1b**. Three different regions designated as 1 to 3 can be well identified in the microstructure (**Figure 1c**). **Figure 1d** shows the typical XRD pattern, which confirms the presence of only two phases such as FCC(A1) and  $\text{L}_{12}$ . **Table 1** summarises the measured average chemical composition of coexisting regions identified by SEM (see **Figure 1c**) in the microstructure of the as-

cast CCA. The region (1) corresponds to the primary FCC(A1) dendrites enriched in Co, Cr, and Fe and depleted in Ni, Al, and Ti compared to those of the average chemical composition of the studied CCA. The region (2) corresponds to the interdendritic region and is enriched in Ni, Al, and Ti and depleted in Cr and Fe compared to those of the average chemical composition. The irregularly shaped particles (3) formed in the centre of the interdendritic region are enriched in Ni, Ti, Al and depleted in Fe and Cr with a stoichiometry corresponding to L<sub>12</sub> - (Ni, Co, Fe, Cr)<sub>3</sub>(Ti, Al) intermetallic phase. The formation of L<sub>12</sub> particles in the interdendritic region is connected with the microsegregation of Al and Ti characterised by partition coefficients  $k_{Al} = 0.91$  and  $k_{Ti} = 0.37$ , respectively, into liquid during solidification [9].

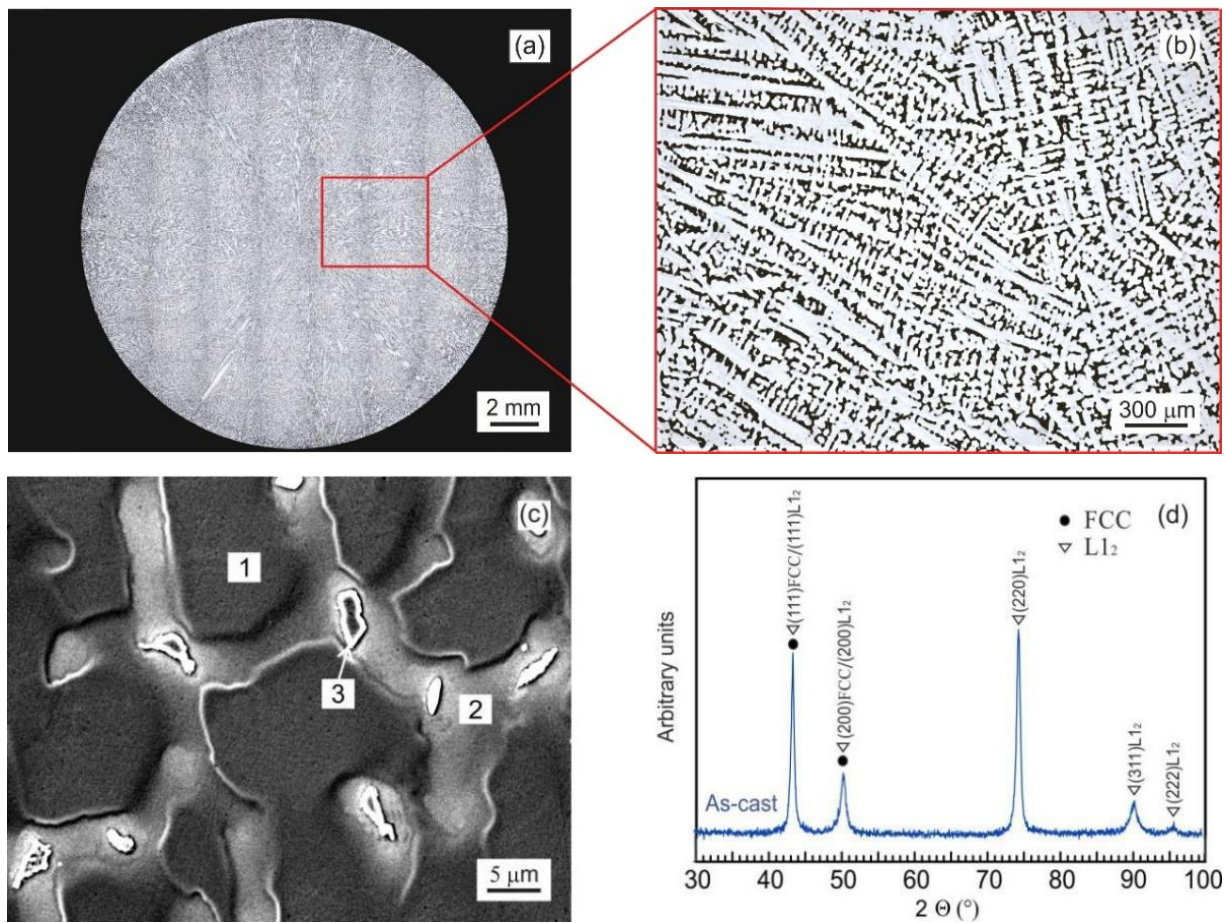


**Figure 1** The typical microstructure of the as-cast CCA: **(a)** LM micrograph of the transversal section of the as-cast ingot; **(b)** LM micrograph showing detail of the microstructure; **(c)** SEM micrograph showing coexisting phase regions, 1 - primary FCC(A1) dendrites, 2 - interdendritic region FCC(A1), 3 - interdendritic L<sub>12</sub> region; **(d)** The typical XRD pattern

**Table 1** Measured chemical composition of coexisting regions and the studied CCAs (at.%).

Region \ Element	Al	Ti	Cr	Fe	Co	Ni
1	2.9 ± 0.3	2.8 ± 0.1	24.5 ± 0.2	24.8 ± 0.2	23.4 ± 0.3	21.6 ± 0.3
2	3.4 ± 0.1	8.3 ± 0.1	21.1 ± 0.6	20.0 ± 0.5	22.2 ± 0.1	25.0 ± 0.3
3	4.9 ± 0.4	22.0 ± 0.1	9.5 ± 0.3	11.2 ± 0.1	22.4 ± 0.3	30.0 ± 0.9
Studied CCA	3.1 ± 0.1	4.6 ± 0.2	23.6 ± 0.4	23.0 ± 0.2	22.7 ± 0.2	23.0 ± 0.3

### 3.2 Microstructure of forged samples

**Figure 2** shows the typical microstructure of the studied CCA after hot forging at 1200 °C. The applied hot forging leads to significant refinement of highly anisotropic coarse columnar grain structure and the formation of isotropic microstructure composed of equiaxed grains, as shown in **Figure 2a**. The forged structure is represented by two types of grains. Besides the large equiaxed grains, the microstructure contains fine grains forming a necklet-type of structure along the grain boundaries, as shown in **Figure 2b**. **Figure 3** shows that the measured statistical data of large grains (about 1000 measurements carried out by an intercept method) fulfil log-normal distribution function characterised by a mean grain size of  $(300 \pm 9) \mu\text{m}$ . The log-normal distribution function for fine grains forming along the grain boundaries results in a mean grain size of  $(20 \pm 4) \mu\text{m}$ . The majority of coarse equiaxed grains contain twins, as seen in **Figure 2a**. The twinning is observed in many high-entropy systems, especially in systems with low stacking-fault energy (SFE). It has been found that the addition of alloying elements significantly reduces the SFE of most materials, which in turn makes the material more likely to be deformed by partial dislocations or twinning [14,15]. The additions of Al and Ti are effective in reducing the SFE of the CoCrFeNi-based alloys because they can induce more considerable deformation of electronic density and make the slipping of atomic layers easier. The present results show that the studied CCA has undergone severe plastic deformation after forging due to the simultaneous action of thermal energy and deformation energy.

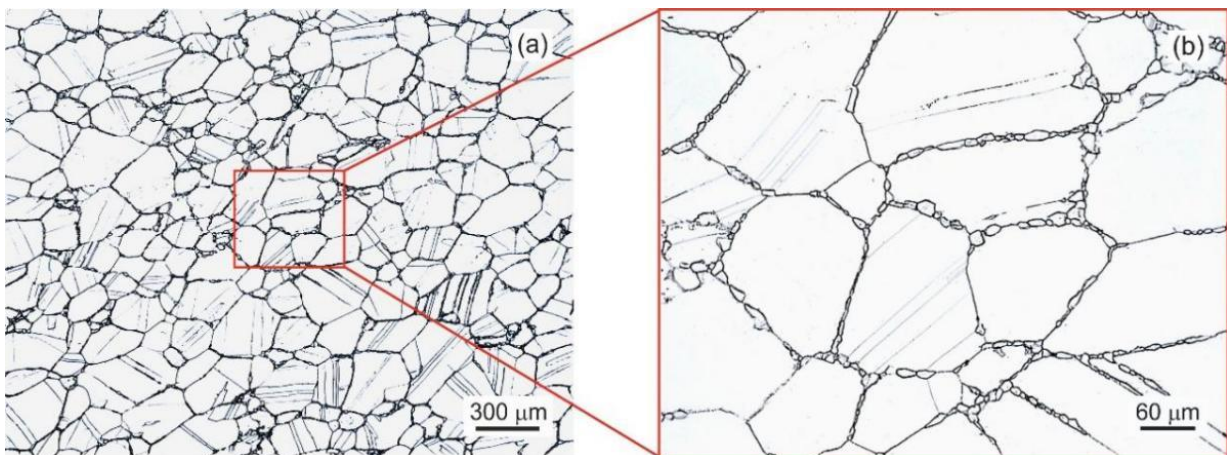


**Figure 2** The typical microstructure of the studied CCA after hot forging at 1200 °C: **(a)** LM micrograph of the longitudinal section of the forged CCA; **(b)** LM micrograph showing detail of the forged microstructure

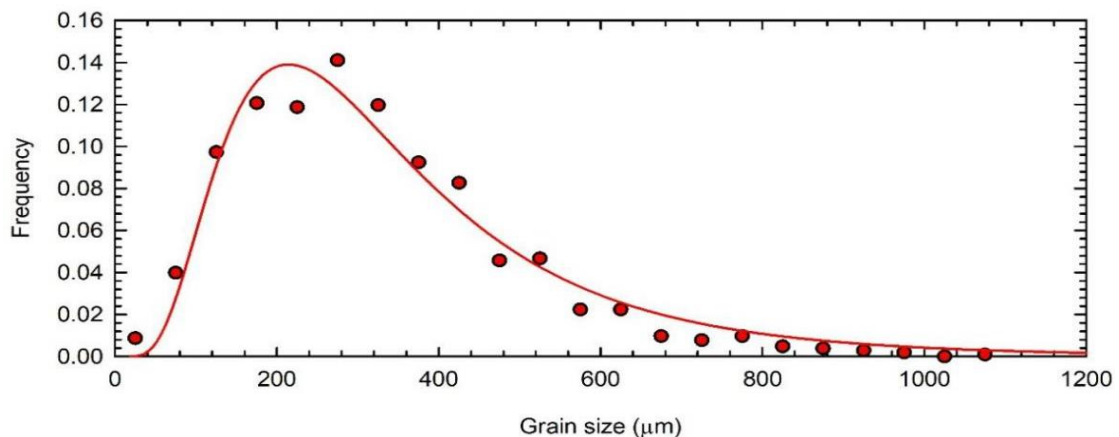


**Figure 3** Log-normal curve showing the distribution of coarse equiaxed grains in the forged CCA alloy

### 3.3 Nanohardness and Vickers microhardness

**Figure 4** shows the results of nanohardness measurements of the coexisting regions identified in the as-cast CCA (see also **Figure 1c**). The nanohardness of the primary FCC(A1) dendrites of 3.4 GPa (region 1) is significantly lower compared to those of 6.0 GPa (region 2) or 8.5 GPa (region 3) measured for FCC(A1) or L<sub>12</sub> phase, respectively.

**Figure 5** shows the effect of the applied thermomechanical heat treatments on the Vickers microhardness of the studied as-cast CCA. The average microhardness of the as-cast CCA is HV<sub>0.05</sub> = 204. However, solution annealing at 1240 °C for 6 h followed up with hot forging at 1200 °C leads to an increase in the microhardness value to HV<sub>0.05</sub> = 260. The annealing at a temperature of 800 °C for 15 h leads to a significant increase in microhardness to a value of HV<sub>0.05</sub> = 388. On contrary, the annealing at a higher temperature of 850 °C for 15 h leads to an increase in microhardness only to HV<sub>0.05</sub> = 350, which indicates a precipitation hardening effect. Such an increase in the microhardness values of the studied CCA subjected to appropriate heat treatments is associated with the formation of the strengthening L<sub>12</sub> precipitates in the FCC(A1) matrix [16-18]. There is a potential that such precipitation-strengthened CCAs with L<sub>12</sub> may be utilized in high-temperature applications, especially since the strengthening ordered intermetallic phases are largely the same as those in present-generation high-temperature nickel-based superalloys alloys [19]. For example, CCAs strengthened with intermetallic particles, like L<sub>12</sub> have the potential to find high temperature applications in aircraft engines.

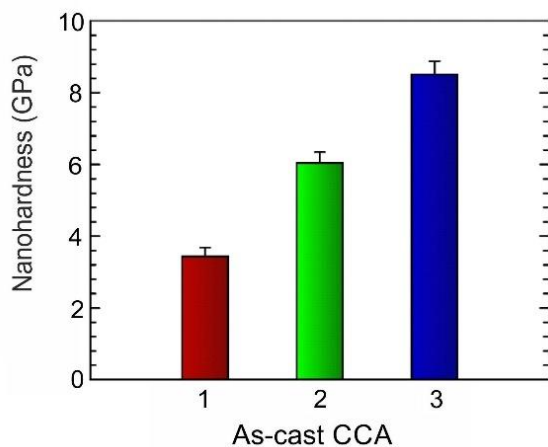


**Figure 4** Nanohardness of different regions identified in the as-cast alloy: 1 - primary FCC(A1) dendrites, 2 - interdendritic FCC(A1), 3 - interdendritic L<sub>12</sub>

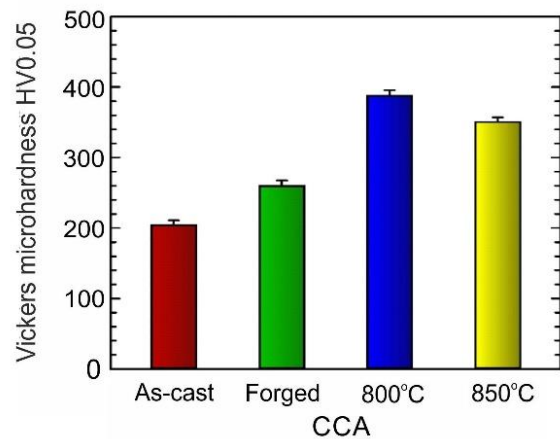


**Figure 5** Vickers microhardness HV<sub>0.05</sub> measured in the as-cast, forged and annealed CCA at 800 and 850 °C

## 4. CONCLUSIONS

In this paper, the preliminary experimental results on the design, processing and selected properties of precipitation hardenable CCA with nominal composition (CoCrFeNi)<sub>92.5</sub>Al<sub>3</sub>Ti<sub>4.5</sub> prepared by vacuum induction melting followed by tilt casting are presented. The precipitation hardening approach has been used to improve room temperature mechanical properties as well as to design a system with the potential working at high temperatures. The minor additions of Ti and Al have been used to promote the formation of a highly dispersed L<sub>12</sub> strengthening phase in FCC(A1) matrix.

The emphasis of this work is on demonstrating how the microstructure of the studied CCA changes during various applied processes. It is shown that the typical microstructure of the as-cast CCA consists of coarse highly anisotropic columnar dendritic grains, which are fully homogenised during solution heat treatment at 1240 °C for 6 h. Hot forging causes the alloy to undergo significant plastic deformation, which in turn leads to grain refinement and the formation of an equiaxed isotropic structure. The chemical and XRD analyses indicate

that the as-cast CCA contains two FCC(A1) solid solutions and intermetallic L<sub>12</sub> particles. The nanohardness of FCC(A1) dendrites is significantly lower compared to those of FCC(A1) or L<sub>12</sub> phases forming in the interdendritic region. An appropriate heat treatment leads to a significant increase in microhardness values due to the precipitation of L<sub>12</sub> particles in FCC(A1) matrix.

## ACKNOWLEDGEMENTS

***This work was financially supported by the Slovak Research and Development Agency under the contracts APVV-20-0505 and the Slovak Grant Agency for Science under the contract VEGA 2/0018/22.***

## REFERENCES

- [1] CANTOR, B., CHANG, I.T.H., KNIGHT, P., VINCENT, A.J.B. Microstructural development in equiatomic multicomponent alloys. *Mater. Sci. Eng. A*. 2004, vol. 375-377, pp. 213-218. Available from: <https://doi.org/10.1016/j.msea.2003.10.257>.
- [2] CANTOR, B. Multicomponent high-entropy Cantor alloys. *Prog. Mater. Sci.* 2020, 100754. Available from: <https://doi.org/10.1016/j.pmatsci.2020.100754>.
- [3] YEH, J.W., CHEN, S.K., GAN, J.Y., LIN, S.J., CHIN, T.S., SHUN, T.T., TSAU, C.H., CHANG, S.Y. Formation of simple crystal structures in Cu-Co-Ni-Cr-Al-Fe-Ti-V alloys with multiprincipal metallic elements. *Metall. Mater. Trans. A*. 2004, vol. 35A, pp. 2533-2536. Available from: <https://doi.org/10.1007/s11661-006-0234-4>.
- [4] GEORGE, E.P., CURTIN, W.A., TASAN, C.C. High entropy alloys: A focused review of mechanical properties and deformation mechanisms. *Acta Mater.* 2020, vol. 188, pp. 435-474. Available from: <https://doi.org/10.1016/j.actamat.2019.12.015>.
- [5] MIRACLE, D.B., MILLER, J.D. SENKOV, O.N., WOODWARD, C., UCHIC, M.D., TILEY, J. Exploration and development of high entropy alloys for structural applications. *Entropy*. 2014. vol. 16, pp. 494-525. Available from: <https://doi.org/10.3390/e16010494>.
- [6] ALI, N., ZHANG, L., LIU, D., ZHOU, SANULLAH, H. K., ZHANG, C., CHU, J., NIAN, Y., CHENG, J. Strengthening mechanisms in high entropy alloys: A review. *Mater. Today Commun.* 2022, vol. 33, 104686. Available from: <https://doi.org/10.1016/j.mtcomm.2022.104686>.
- [7] MISHRA, R.S., HARIDAS, R.S., AGRAWAL, P. High entropy alloys - Tunability of deformation mechanisms through integration of compositional and microstructural domains. *Mater. Sci. Eng. A*. 2021, vol. 812, 141085. Available from: <https://doi.org/10.1016/j.msea.2021.141085>.
- [8] GORSSE, S., COUZINIÉ, J.P., MIRACLE, D.B. From high-entropy alloys to complex concentrated alloys. *Comptes Rendus Phys.* 2018, vol.19, pp. 721-736. Available from: <https://doi.org/10.1016/j.crhys.2018.09.004>.
- [9] LAPIN, J., KLIMOVA, A., PELACHOVA, T., ŠTAMBORSKÁ, M., BAJANA, O. Synergistic effect of Ti, B, Si, and C on microstructure and mechanical properties of as-cast Al<sub>0.4</sub>Co<sub>0.9</sub>Cr<sub>1.2</sub>Fe<sub>0.9</sub>Ni<sub>1.2</sub>(Si, Ti, C, B)<sub>0.375</sub> complex concentrated alloy. *J. Alloys Compd.* 2023. vol. 934, 168050. Available from: <https://doi.org/10.1016/j.jallcom.2022.168050>.
- [10] ŠTAMBORSKÁ, M., LAPIN, J. Effect of anisotropic microstructure on high-temperature compression deformation of CoCrFeNi based complex concentrated alloy. *Kov. Mater.* 2017, vol. 55, pp. 369-378. Available from: [https://doi.org/10.4149/km\\_2017\\_6\\_369](https://doi.org/10.4149/km_2017_6_369).
- [11] GORSSE, S., MIRACLE, D.B. SENKOV, O.N. Mapping the world of complex concentrated alloys. *Acta Mater.* 2017, vol. 135, pp. 177-187. Available from: <https://doi.org/10.1016/j.actamat.2017.06.027>.
- [12] LAPIN, J., MAKWANA, M., KLIMOVA, A. Effect of heat treatments on microstructure and mechanical properties of Al<sub>0.5</sub>CoCrFeNi complex concentrated alloy. *Kov. Mater.* 2021, vol. 59, pp. 79-91. Available from: [https://doi.org/10.4149/km\\_2021\\_2\\_79](https://doi.org/10.4149/km_2021_2_79).
- [13] HE, J.Y., WANG, H., WU, Y., LIU, X.J., MAO, H.H., NIEH, T.G., LU, Z.P. Precipitation behavior and its effects on tensile properties of FeCoNiCr high-entropy alloys. *Intermetallics*. 2016, vol. 79, pp. 41-52. Available from: <https://doi.org/10.1016/j.intermet.2016.09.005>.

- [14] LI, X., SCHÖNECKER, S., VITOS, L., LI, X. Generalized stacking faults energies of face-centered cubic high-entropy alloys: A first-principles study. *Intermetallics*. 2022, vol.145, 107556. Available from: <https://doi.org/10.1016/j.intermet.2022.107556>.
- [15] LIU, S.F., WU, Y., WANG, H.T., HE, J.Y., LIU, J.B., CHEN, C.X., LIU, X.J., WANG, H., LU, Z.P. Stacking fault energy of face-centered-cubic high entropy alloys. *Intermetallics*. 2018, vol. 93, pp. 269-273. Available from: <https://doi.org/10.1016/j.intermet.2017.10.004>.
- [16] FANG, J.Y.C., LIU, W.H., LUAN, J.H., YANG, T., WU, Y., FU, M.W., JIAO, Z.B. Competition between continuous and discontinuous precipitation in L1<sub>2</sub>-strengthened high-entropy alloys. *Intermetallics*. 2022, vol. 149, 107655. Available from: <https://doi.org/10.1016/j.intermet.2022.107655>.
- [17] LU, Y., ZHANG, ZHAO, K., DONG, B. X., SUN, F., ZHOU, B., ZHEN, Y., ZHANG, L. Balanced mechanical properties of Al<sub>0.3</sub>CoCrFeNiTi<sub>x</sub> high-entropy alloys by tailoring Ti content and heat treatment. *Mater. Sci. Eng. A*. 2023, vol. 866, 144677. Available from: <https://doi.org/10.1016/j.msea.2023.144677>.
- [18] FANG, J.Y.C., LIU, W.H., LUAN, J.H., YANG, T., FU, M.W., JIAO, Z.B. Dual effects of pre-strain on continuous and discontinuous precipitation of L1<sub>2</sub>-strengthened high-entropy alloys. *J. Alloys Compd.* 2022, vol. 925, 166730. Available from: <https://doi.org/10.1016/j.jallcom.2022.166730>.
- [19] KNOWLES, A.J., REYNOLDS, L., VORONTSOV, V.A, DYE, D. A nickel based superalloy reinforced by both Ni<sub>3</sub>Al and Ni<sub>3</sub>V ordered - fcc precipitates. *Scripta Materialia*. 2019, vol. 162, pp. 269–273. Available from: <https://doi.org/10.1016/j.scriptamat.2018.12.013>.